DOI: 10.1002/ejic.201001201

A Combined Experimental and Theoretical Study on Bis(μ-alkoxo)diiron(III) Complexes with Hydroxybenzylaminoethanol [O,N,O] Donor Ligands: Syntheses, Structures and Magnetic Properties

Mikko M. Hänninen,[a] Enrique Colacio,*[b] Antonio J. Mota,[b] and Reijo Sillanpää*[a]

Keywords: Iron / Magnetic properties / DFT calculations / Structure elucidation

Three new neutral bis(μ-alkoxo)diiron(III) complexes were prepared from *N*(R),*N*-(2-methylene-4,6-di-*tert*-butylphenol)aminoethan-1-ol ligands (H_2L1, R = Me and H_2L2, R = H). In these complexes, the ligand wraps around the metal center exhibiting a tridentate facial coordination mode with alkoxo-bridging oxygen, amine nitrogen and phenoxo oxygen donor atoms. In the complex $[Fe(acac)L1]_2$·MeCN (**1**) acetylacetonato coligand complete the distorted octahedral coordination spheres of the iron(III) ions, whereas in the five-coordinate iron(III) chloride complexes $[FeClL1]_2$ (**2**) and $[FeClL2]_2$ (**3**) the ligands induce a geometry that is intermediate between square pyramidal and trigonal bipyramidal. Magnetic studies carried out on these dinuclear complexes showed that *J* values vary from –16.1 to –29.6 cm^{-1}. Both experimental and theoretical DFT studies address a strong magneto-structural correlation between the exchange coupling constant and the Fe–O–Fe angle of the complexes. The crossover point from antiferromagnetic to ferromagnetic coupling is predicted to be 100.4° for this family of *N*(R),*N*-(2-methylene-4,6-di-*tert*-butylphenol)aminoethan-1-ol ligands.

Introduction

Oxygen-bridged diiron(III) complexes have attracted much attention during the last few decades due to their biological relevance as functional and structural models for various non-heme proteins such as hemerytrin and methane monooxygenase.[1] Because of these bioinorganic implications, oxygen-bridged diiron(III) complexes have been the subject of many magnetic studies aimed to establish magneto-structural correlations. Thus, a nice correlation was established by Le Gall et al. between *J* and the Fe–O–Fe angle for a family of planar binuclear $Fe(O)_2Fe$ complexes with β-diketonate-alkoxide peripheral ligands.[2] However, other oxygen-bridged diiron(III) complexes do not obey this correlation. The same can be ascribed for the semiempirical correlation established by Gorum and Lippard[3] and further refined by Haase et al.[4] between *J* and the coupling distance P, defined as half the shortest superexchange pathway between the two Fe^{III} ions. More recently, Haase et al.[4] obtained an equation applying the angular and radial overlap model, that, however, did not improve the *J* values calculated by the semiempirical Gorum and Lippard's equation. It seems that the success of a particular equation is tied to the nature of the oxygen-bridged diiron(III) complexes. In view of this, we decided to prepare three new examples of dialkoxo-bridged diiron(III) complexes with two closely related hydroxybenzylaminoethanol polydentate ligands (Figure 1) and different anionic ancillary ligands (acetylacetonate and chloride anions). The aim is to investigate if the correlation between *J* and either the Fe–O distance or the Fe–O–Fe angles could be operative in this family of compounds. These results might help to know which are the most important factors governing the value of *J* in each type of alkoxo-bridged diiron(III) complexes. This information would be very useful to deliberately prepare Fe_2 "molecular bricks" with predefined magnetic properties, which could be used in the construction of high nuclearity clusters that eventually could exhibit single-molecule magnet (SMM) behaviour.[5]

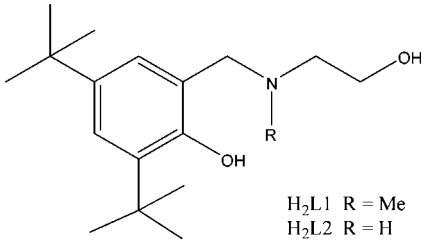

Figure 1. Schematic representation of ligands H_2L1 and H_2L2.

Results and Discussion

The *N*(R),*N*-(2-methylene-4,6-di-*tert*-butylphenol)aminoethan-1-ol ligands H_2L1 (R = Me) and H_2L2 (R = H) were

[a] Department of Chemistry, University of Jyväskylä,
P. O. Box 35, 40014 Jyväskylä, Finland
E-mail: resillan@jyu.fi
[b] Departamento de Química Inorgánica, Facultad de Ciencias, Universidad de Granada,
Avda. Fuentenueva s/n, 18002 Granada, Spain
Supporting information for this article is available on the WWW under http://dx.doi.org/10.1002/ejic.201001201.

prepared by a novel solvent-free Mannich-type condensation reaction. The flexible backbone of these hydroxybenzylaminoethanol polydentate ligands should allow more versatile coordination chemistry than their more frequently used Schiff's base counterparts. When fully deprotonated, these ligands could act as tridentate anionic ligands capable to coordinate iron(III) ions in a chelating/bridging fashion. When H_2L1 and H_2L2 were allowed to react with either $Fe(acac)_3$ and/or $FeCl_3$, the bis(μ-dialkoxo)diiron(III) complexes $[Fe(acac)L1]_2$·MeCN (**1**), $[FeL1]_2$ (**2**) and$[FeClL2]_2$ (**3**) were obtained in moderate yields. In addition, few crystals of complex **4S** (Figure S1) were obtained when the solution of ligand H_2L3 (Figure S1) and $Fe(acac)_3$ was evaporated to dryness. The attempts to prepare this compound on a larger scale were unsuccessful; hence other experimental data of the compound are absent. A detailed description of the syntheses of **1**–**3** can be found in the Exp. Section.

Solid State Structures of Complexes 1–3

The molecular structure of complex **1** is shown in Figure 2 and the relevant bond lengths and angles are presented in Table 1. The complex **1** consists of neutral $[Fe(acac)L1]_2$ molecules of C_i symmetry and a non-coordinating acetonitrile molecule per each dinuclear iron(III) unit. The fully deprotonated $L1^{2-}$ ligand wraps around the metal center exhibiting a tridentate facial coordination mode with alkoxo-bridging oxygen, amine nitrogen and phenoxo oxygen donor atoms, leading to a [Fe(μ-alkoxo)$_2$] rhombus-shaped core. The oxygen donor atoms of the acetylacetonato coligand complete the distorted octahedral FeO_5N coordination environment of each iron(III) center. The distortion from the octahedral geometry is mainly caused by the strained five-membered ring formed by the metal center and the –N–CH_2–CH_2–O– fragment of the ligand [bite angle of 77.8(1)°], which forces the N8–Fe1–$O2^i$ angle to bend over 25° from the optimal value of 180°. Fe–O(acac) bond lengths are comparable to those found in $Fe(acac)_3$ species[6] with slightly longer values for Fe–O3 (*trans* to Fe–O1 bond) than for Fe–O4 (*trans* to Fe–O2 bond), thus indicating a stronger Fe–O(phenolate) bond interactions in comparison to the Fe–O(ethanolate bridging) bond. In general, the Fe–O, Fe–N bond lengths and Fe–Fe separation are in good agreement with earlier studies.[7]

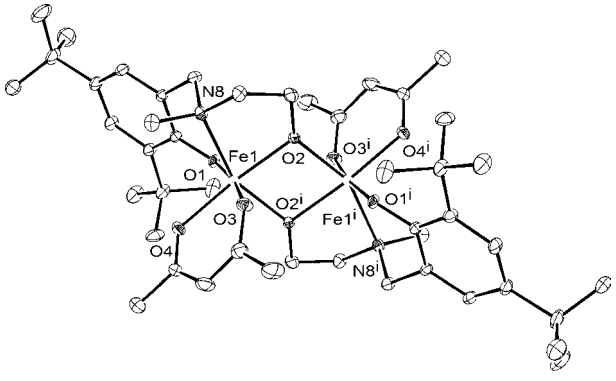

Figure 2. Molecular structure of $[Fe(acac)L1]_2$ unit in (**1**); symmetry operation i: 1 – *x*, 1 – *y*, 1 – *z*. Thermal ellipsoids are drawn at 30% probability level; hydrogen atoms and non-coordinating acetonitrile molecule are omitted for clarity.

Table 1. Selected bond lengths [Å] and angles [°] for **1**.[a]

Fe1–N8	2.195(3)	O1–Fe1–O2	102.7(1)
Fe1–O1	1.901(3)	O2–Fe1–$O2^i$	76.7(1)
Fe1–O2	2.028(3)	N8–Fe1–O2	77.8(1)
Fe1–$O2^i$	1.964(3)	N8–Fe1–$O2^i$	154.3(1)
Fe1–O3	2.093(3)	O1–Fe1–$O2^i$	99.1(1)
Fe1–O4	2.003(3)	Fe1–O2–$Fe1^i$	103.3(1)
Fe1–$Fe1^i$	3.1311(9)		

[a] Symmetry operation i: 1 – *x*, 1 – *y*, 1 – *z*.

Complex **2** crystallizes in the monoclinic space group $P2_1/c$, with two halves of distinct dinuclear iron(III) complexes in the asymmetric unit forming neutral centrosymmetric $[FeClL1]_2$ molecules in the unit cell. Although there are small differences in the geometrical parameters around the two different Fe-centers, the coordination spheres and most of the bond lengths and angles are similar, hence structural discussion concentrates on the Fe1–$Fe1^i$ centrosymmetric unit depicted in Figure 3 (a). The selected bond lengths and angles are presented in Table 2.

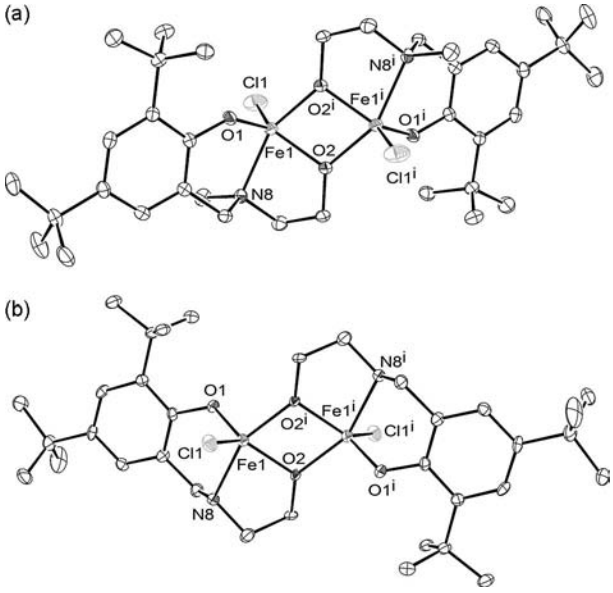

Figure 3. (a) molecular structure of one $[FeClL1]_2$ unit in **2**; symmetry operation i: 1 – *x*, –*y*, 2 – *z*. (b) Molecular structure of one $[FeClL2]_2$ in **3**; symmetry operation i: –*x*, 1 – *y*, 1 – *z*. Thermal ellipsoids are drawn at 30% probability level and all hydrogen atoms are omitted for clarity.

The tridentate bridging $L1^{2-}$ ligand settles around the metal ion in the same manner as in complex **1** forming two alkoxo bridges between the two iron(III) centers. A chloride anion occupies the vacant site producing a neutral complex where each iron atom exhibits a $FeNO_3Cl$ coordination environment with a geometry intermediate between trigonal bipyramidal (TBPY-5) and square pyramidal (SPY-5). To estimate the distortion of the coordination polyhedron, the

Table 2. Selected bond lengths [Å] and angles [°] for **2a**, **2b**, **3a** and **3b**.[a]

	2a	2b	3a	3b
Fe–N8	2.192(2)	2.179(2)	2.134(7)	2.146(7)
Fe–O1	1.822(2)	1.835(2)	1.831(5)	1.834(5)
Fe–O2	1.955(2)	1.949(2)	1.974(5)	1.948(5)
Fe–O2^{i} [b]	1.997(2)	1.986(2)	1.977(5)	1.969(5)
Fe–Cl1	2.2155(9)	2.218(1)	2.255(2)	2.237(3)
Fe–Fe^{i}	3.1376(5)	3.1128(6)	3.143(2)	3.125(2)
O1–Fe–O2	122.04(9)	121.55(9)	119.9(2)	123.9(2)
O2 – Fe–O2^{i}	74.87(8)	75.46(9)	74.6(2)	74.2(2)
N8–Fe–O2	78.75(8)	79.51(9)	77.8(2)	79.3(2)
N8–Fe–O2^{i}	153.19(8)	154.05(9)	152.4(2)	153.3(2)
O1–Fe–O2^{i}	100.93(9)	96.16(9)	103.5(2)	100.9(2)
Fe–O2–Fe^{i}	105.13(9)	104.5(1)	105.4(2)	105.8(2)

[a] The numbers under **2a**, **2b** and **3a**, **3b** are related to the bond parameters around Fe1 and Fe2 molecules in the asymmetric unit. [b] Symmetry codes i for **2a**, **2b**, **3a** and **3b** are $2 - x$, $1 - y$, $2 - z$; $1 - x$, $-y$, $2 - z$; $1 - x$, $-y$, $1 - z$; $-x$, $1 - y$, $1 - z$, respectively.

method of Addison and Rao[8] was used to calculate the δ values for the metal centers. The analysis of the coordination sphere of the complexes units in **2** around Fe1 and Fe2 units gives δ values of 0.54 and 0.52, respectively, which indicate that the geometry is almost at the middle of the TBPY-SPY deformation pathway. In the SPY-5 description, the O2, O2^{i}, N8 and O1 atoms are located in the basal positions whereas the chloride anion occupies the apical position. On the other hand, in the TBPY-5 description, the equatorial positions are occupied by the O1, O2 and Cl atoms and the axial positions by the N8 and O2i atoms.

Complex **3** crystallizes in the centrosymmetric triclinic space group $P\bar{1}$ (Figure 3, b). Selected bond lengths and angles are presented in Table 2. The molecular structure of the two dinuclear units in **3** is quite similar to those in **2**. As in **2**, the geometry of each $FeNO_3Cl$ coordination polyhedron is intermediate between TBPY-5 and SPY-5 (δ = 0.49 and 0.54 for Fe1 and Fe2, respectively).

In complexes **1**–**3** the intermolecular interactions are minimal due to the presence of bulky *tert*-butyl substituents in the phenyl rings of the ligands. Thus, neither hydrogen bonds nor π-π interactions are present in the complexes and the interdinuclear Fe···Fe distances are in general over 7 Å.

Magnetic Properties

The temperature dependence of $\chi_M T$ (χ_M is the molar magnetic susceptibility per Fe_2 unit) of **1**–**3** in the range 300–2 K are shown in Figure 4. The $\chi_M T$ product at room temperature (6.59, 6.29 and 5.9 $cm^3 mol^{-1} K$ for **1**, **2** and **3**, respectively) is lower than that expected for two uncoupled $S = 5/2$ with $g = 2.0$ (8.75 $cm^3 mol^{-1} K$), thus indicating the existence of a moderate to strong antiferromagnetic coupling in these compounds.

The χ_M vs. T plots show a wide maximum in the 55–85, 80–120, and 100–125 K range for **1**, **2** and **3**, respectively. Below the temperature of the maximum, χ_M decreases with decreasing the temperature and, in the case of **2** and **3**, at very low temperature, χ_M increases, which indicates the

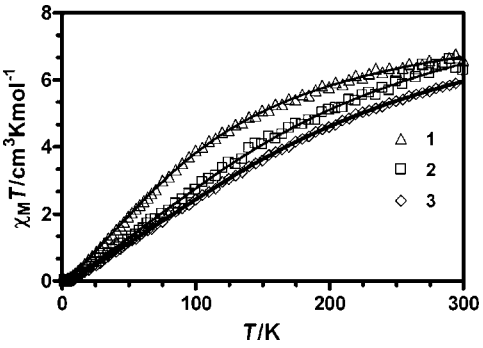

Figure 4. Temperature dependence of the $\chi_M T$ for **1**–**3**.

presence of a small amount of paramagnetic impurity. This behaviour supports the antiferromagnetic interaction between the iron(III) atoms leading to an S = 0 ground state. Magnetic susceptibility data were analyzed with the isotropic Hamiltonian $\boldsymbol{H} = -J\boldsymbol{S_1}\boldsymbol{S_2} + g\beta(\boldsymbol{S_1} + \boldsymbol{S_2})H$. The energy levels derived from this Hamiltonian were introduced in the van Vleck equation to obtain the following theoretical Equation (1).

$$\chi_M = \frac{Ng^2\beta}{kT}\frac{2\exp x + 10\exp 3x + 28\exp 6x + 60\exp 10x + 110\exp 15x}{1 + 3\exp x + 5\exp 3x + 7\exp 6x + 9\exp 10x + 11\exp 15x}(1-\rho) + 2.1875g^2\rho \quad (1)$$

A ρ parameter was included in the theoretical equation to account for the percentage of paramagnetic impurity. The best fit of the experimental data to the theoretical equation led to the following parameters: $J = -16.1(1)$ cm^{-1} and $g = 2.001(3)$ for **1**, $J = -27.2(5)$ cm^{-1} and $g = 2.15(1)$ and $\rho = 0.003(2)$ for **2** and $J = -29.6(2)$ cm^{-1} and $g = 2.105(4)$ and $\rho = 0.0041(5)$ for **3**. The J values for **2** and **3** are among the highest found for bis(μ-dialkoxo)diiron(III) complexes.[4]

DFT calculations of the magnetic exchange coupling carried out on the molecular structures as found in the solid state predicts J values for **1**–**3** (see Table 3) which are close to those obtained from the experimental susceptibility data. The calculations were performed also for complex **4S** and the obtained values are in line with the similar complex **1** (Table S1). J values are calculated taking into account that the difference between the high-spin state (of multiplicity 11) and the broken-symmetry singlet state is equal to $-15J$.

Table 3. Calculated and experimental J values for **1**–**3**.

	J_{cal} [cm^{-1}]	J_{exp} [cm^{-1}]	Fe–O–Fe [°]	Fe–O_{av} [Å]	τ [°]	J_{eq1}/cm^{-1} [c]
1	–15.8	–16.1	103.33	1.996	21	–9.64
2	–21.5[a]	–27.2	104.54	1.9675	2.5	–14.3
	–23.3[b]		105.13	1.9760	14.8	–12.7
3	–26.5[a]	–29.6	105.41	1.9755	1.9	–12.8
	–28.9[b]		105.83	1.9585	10.5	–16.2

[a] Dinuclear unit a. [b] Dinuclear unit b. [c] Values obtained from Equation (1).

In 1991, Gorum and Lippard[3] were able to establish a semiempirical correlation for dinuclear oxygen-bridged iron(III) complexes with double or triple bridges (OR^-,

OPh$^-$, OH$^-$ and three-atomic bridging anions of the type O_2X^- like acetate, nitrate, etc.). They showed that the exchange coupling constant, *J*, could be correlated with the half of the length of the shortest Fe–O–Fe bridge in the complex (*P*) as follows [Equation (2)]

$$J = A\exp[B\,P(\text{Å})] \quad (2)$$

with $A = -8.763 \times 10^{10}$ cm^{-1} and $B = -12.663$ Å^{-1}. Later on, using an expanded collection of data for double oxygen-oxygen-bridged dinuclear iron(III) complexes, Haase et al.[4] obtained the following improved coefficients ($A = -1.08 \times 10^{13}$ cm^{-1} and $B = -13.9$ Å^{-1}). However, *J* values for bis(μ-hydroxo) and bis(μ-alkoxo)diiron(III) complexes were not well reproduced by Equation (1). In view of this, Haase et al.,[4] following a strategy previously used by Weihe and Güdel for single-oxo-bridged diiron(III) complexes,[9] obtained an equation that takes into account a radial as well as an angular dependence of the exchange parameter for symmetrically bridged complexes. However, application of this angular and radial overlap model did not improve the *J* values calculated by the semiempirical Equation (2). Therefore, they concluded that the magnitude of the Fe–O–Fe angle had not any noticeable influence on the exchange coupling. This fact was explained by considering that, for the spherical distribution of the high-spin d^5 ions, the angular dependences of the overlap integral for the several exchange pathways in the dinuclear iron(III) complex compensate each other in such a way that the resulting exchange interaction shows no pronounced angle dependence. In view of this, we have used the improved *A* and *B* values into Equation (2) to determine the *J* values for **1**–**3**. However, the calculated values (see Table 3) are far from the experimental ones. It should be noted that for planar double-bridged $Fe(OR)_2Fe$ complexes, such as **1**–**3** the exchange pathway involving the $d_{x^2-y^2}/d_{x^2-y^2}$ orbitals should be the most effective in mediating the magnetic exchange interaction. In this case, not only the Fe–O distance but also the Fe–O–Fe angle should have a significant influence on the magnetic exchange coupling. We have found, by analyzing a large amount of planar $Fe(OR)_2Fe$ complexes, that there exists a correlation between the Fe–O distance and the Fe–O–Fe angle: the smaller the Fe–O–Fe angle the longer is the Fe–O distance. Complexes **1**–**3** follow this trend as can be observed in Table 3. If these two structural parameters are correlated, in principle, it should be possible to establish a magneto-structural correlation based on one of these structural parameters. Thus, even though the calculated *J* values and the average Fe–O distances for **1**–**3** data can be fitted to a straight line (Figure 5), the $r^2 = 0.72$ value is not good. There exists, however, a good linear relationship between the calculated *J* values and the Fe–O–Fe angle values with $r^2 = 0.97$.

This result shows that for this family of planar $Fe(OR)_2Fe$ complexes the main structural factor governing the sign and magnitude of the magnetic exchange coupling is the Fe–O–Fe angle. It should be noted that neither the τ angle [out-of-plane shift of the carbon atom with respect to the $Fe(O)_2Fe$ plane] nor the Fe···Fe distance seems to have any

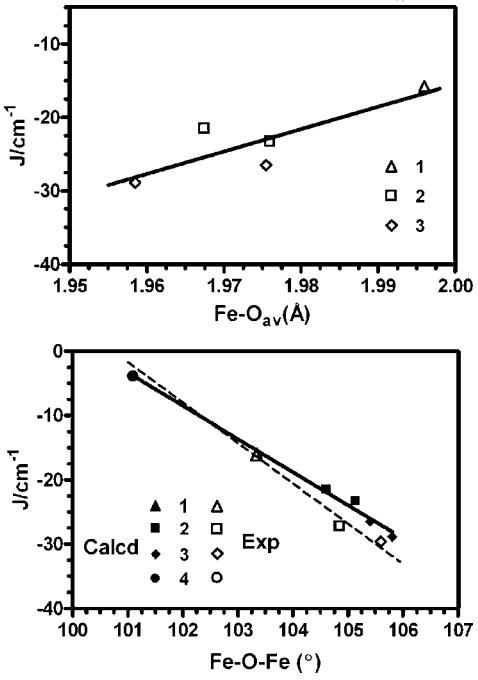

Figure 5. Plots of the calculated *J* vs. the average Fe–O distance (top) and the Fe–O–Fe angle (bottom). Calculated and experimental values are represented by circles and triangles, respectively.

clear influence on the magnetic exchange coupling. Moreover, as expected from the spherical distribution of high-spin d^5 ions, the coordination geometry of the iron(III) ions (distorted octahedral for **1** and intermediate between square-pyramidal and trigonal-bipyramidal for **2** and **3**) has not any direct effect on *J* either. From the linear correlation between *J* and the Fe–O–Fe angle, the crossover point from AF to F interactions is predicted at 100.4° for this family of *N*(R),*N*-(2-methylene-4,6-di-*tert*-butylphenol)aminoethan-1-ol ligands. It should be noted that there exists also a good linear relationship between the experimental *J* values and the Fe–O–Fe angles, also with $r^2 = 0.97$ (see Figure 5). Notice that in two cases, compounds **2** and **3**, the Fe–O–Fe angle actually is the average value for two crystallographically independent molecules, which may introduce some degree of uncertainty in the *J* vs. Fe–O–Fe correlation. We and others have previously found that for planar bis(phenoxo)-bridged copper(II) complexes the main structural factor governing the sign and magnitude of the magnetic exchange coupling is the Cu–O–Cu angle.[10]

As far as we know, no examples of ferromagnetic coupled planar $Fe(OR)_2Fe$ complexes have been reported so far that could support that prediction. Nevertheless, the fact that the experimental and calculated *J* values for the complex $[Fe_2(bbpnol)_2]$ [H_3bbpnol = *N*,*N*-bis(2-hydroxybenzyl)-2-hydroxy-1,3-propanediamine][7b] **4** ($J_{exp} = -2.2$ cm^{-1} and $J_{cal} = -3.9$ cm^{-1}), which contains a ligand similar to those existing in complexes **1**–**3** and a smaller Fe–O–Fe angle (101.1°), fully obey the *J* vs. Fe–O–Fe linear relationships depicted in Figure 5 (the correlation is improved on considering also the structure **4S**: $r^2 = 0.99$ for both experimental and calculated *J* values and the crossover point from AF

Table 4. Spin density for compounds **1**–**3**.

	Fe1	Fe1^{i}	O2	O2^{i}	O1	O1^{i}	N8	N8^{i}	Cl1	Cl1^{i}	O3acac	O4acac
1	+4.2010	–4.2010	+0.0193	–0.0194	+0.2167	–0.2168	+0.0934	–0.0934	–	–	+0.0760	–0.0760
2a	+4.0953	–4.0952	–0.0414	+0.0414	+0.2635	–0.2635	+0.1031	–0.1031	+0.2213	–0.2213	–	–
2b	–4.0827	+4.0827	+0.0387	–0.0384	–0.2769	+0.2766	–0.1036	+0.1036	–0.2208	+0.2208	–	–
3a	–4.0865	+4.0865	+0.0285	–0.0286	–0.2827	+0.2831	–0.1074	+0.1074	–0.2124	+0.2122	–	–
3b	–4.0913	+4.0912	+0.0275	–0.0278	–0.2719	+0.2723	–0.0972	+0.0972	–0.2273	+0.2273	–	–

to F interactions remains at 100.4° for the calculated *J* values) seems to support the goodness of the predicted crossover point value for this family of complexes containing hydroxybenzylaminoethanol ligands.

The calculated spin density for the ground singlet state of **1**–**3** are given in Table 4 (the spin density for **1** and **2** are shown in Figure 6, whereas the spin density for **3**, which is very similar to that of **2** is given in the Supporting Information) and offer information on the electronic structure and the mechanism of the magnetic exchange interaction.

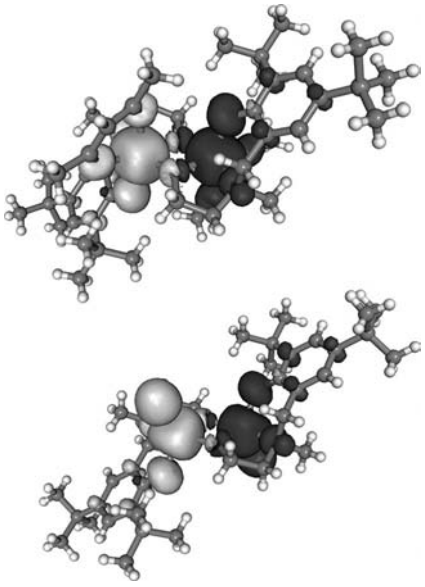

Figure 6. Calculated spin density distribution for the singlet broken-symmetry state of **1** (top) and **2a** (down). Light grey and dark grey shapes correspond to positive and negative spin densities, respectively. The isodensity surface corresponds to a cut-off value of 0.002 e bohr^{-3}.

The shape of the Fe^{III} atoms is quasi spherical as expected for a set of five *d* orbitals with one unpaired electron on each. The sphere is somewhat flattened in the directions of the metal-ligand bonds and small spin densities of the same sign appear on the ligands. This loss of sphericity at the Fe^{III} atoms is the result of the smaller spin density at the e_g orbitals than at the t_{2g} orbitals, which is a consequence of the significant spin density delocalization for the σ-type e_g orbitals to the donor atoms of the ligand.[11] As expected, the delocalization is more important for the atoms directly bound to the Fe^{III} atoms. Nevertheless, the spin density delocalized on the oxygen atoms of the bridging region is always significantly smaller than those on the phenolate oxygen atoms and chloride ligands. Anyway, the spin density is mainly found at the metal, as expected if they are the magnetic centers. It should be noted that the spin density on the Fe^{III} ions in **1** is higher than in **2** and **3**, which indicates that the spin density is less delocalized for the former. This is in agreement with the fact that compound **1** exhibits the smaller AF coupling.

Conclusions

We have prepared three novel dinuclear μ-dialkoxo-bridged iron(III) complexes and examined their solid-state structures and magnetic properties. We have found that a magneto-structural correlation exists between both the experimental and calculated *J* values and the Fe–O–Fe angle for these complexes. It should be noted that such a strong correlation does not exist with other structural parameters (e.g. Fe–O or Fe···Fe distances), hence the main structural factor governing the magnetic exchange coupling between planar $Fe(OR)_2Fe$ complexes is proven to be the Fe–O–Fe angle. The crossover point from AF to F interactions is predicted at 100.4°. It should be noted that no examples of ferromagnetic coupled planar $Fe(OR)_2Fe$ complexes have been reported so far that could support that prediction. Therefore, experimental efforts aimed to prepare this kind of compounds are required. The use of the same family of *N*(R),*N*-(2-methylene-4,6-di-*tert*-butylphenol)aminoethan-1-ol ligands together with bidentate anions (acetate, benzoate, etc) that can also bridge the iron(III) ions, may lead to planar $Fe(OR)_2Fe$ complexes with smaller Fe–O–Fe angles and ferromagnetic exchange interactions. Work along this line is currently undertaken in our lab.

Experimental Section

General: Starting materials for all syntheses were purchased from Aldrich, Merck or Riedel and were of reagent grade and used as received. Solvents were of HPLC grade and dried with 4 Å molecular sieves prior to use. All syntheses were performed under ambient laboratory atmosphere. $Fe(acac)_3$ was prepared according to literature.[12] The NMR spectra of the ligands were recorded with a Bruker Avance DPX 250 FTNMR spectrometer. The ^{1}H NMR spectra were recorded in $CDCl_3$ at 30 °C. The chemical shifts are reported in ppm and referenced internally by using the residual protic solvent resonances relative to tetramethylsilane CDCl: δ = 7.26 ppm. Elemental analysis was performed by using a Vario El III elemental analyzer. HPLC measurements were made with a Perkin–Elmer series 200 equipment [column: Phenomenex Luna 5u C18 250 × 4.60 mm, solvent: 97.5% methanol, 2% water and 0.5% tris(hydroxymethyl)aminomethane, flow rate 2 mL/min, λ = 254 nm]. Single-crystal X-ray measurements were performed by using an Enraf Nonius Kappa CCD area detector diffractometer

with the use of graphite monochromated Mo-K_α radiation. Variable-temperature (2–300 K) magnetic susceptibility measurements on polycrystalline samples were carried out with a Quantum Design Squid MPMSXL-5 device operating at 1 T from room temperature to 50 K and at 0.05 T from this latter temperature to 2 K. The experimental susceptibilities were corrected for the diamagnetism of the constituent atoms by using Pascal's tables.

Ligand and Complex Synthesis: Ligands H_2L1 and H_2L2 were synthesized following a general procedure[13] as follows: 11 mmol of 2,4-di-*tert*-butylphenol, 11 mmol of paraformaldehyde and 10 mmol of the corresponding amine (*N*-methylethanolamine or 2-aminoethanol, respectively) were placed in a partially closed reaction vial. The vial was kept in thermal oven (120 °C) and the reaction was monitored with HPLC. When the reaction finished (judged by disappearance of the starting materials by HPLC) the formed yellow oil was dissolved in acetonitrile. Concentrated HCl(aq.) was added to the solution until the corresponding ligand hydrochloride precipitated. The precipitate was filtered, washed with acetonitrile and neutralized with $NaHCO_3$ (aq.) to yield the *N*(R),*N*-(2-methylene-4,6-di-*tert*-butylphenol)aminoethan-1-ol ligand.

H_2L1: Yield 2.51 g (86%), ^{1}H NMR (250 MHz, CDCl3): δ = 1.30 [s, 9 H, aryl-C(CH_3)$_3$], 1.43 [s, 9 H, aryl-C(CH_3)$_3$], 2.40 (s, 3 H, NCH_3), 2.68 (t, 2 H, NCH_2CH$_2$OH), 3.75 (s, 2 H, aryl-CH_2-N), 3.78 (t, 2 H, NCH$_2$CH_2OH), 6.84 (d, 1 H, Ar*H3*), 7.24 (d, 1 H, Ar*H5*) ppm.

H_2L2: Yield 1.43 g (51%), ^{1}H NMR (250 MHz, CDCl3): δ = 1.29 [s, 9 H, aryl-C(CH_3)$_3$], 1.43 [s, 9 H, aryl-C(CH_3)$_3$], 2.86 (t, 2 H, NCH_2CH$_2$OH), 3.78 (t, 2 H, NCH$_2$CH_2OH), 4.00 (s, 2 H, aryl-CH_2-N), 6.88 (d, 1 H, Ar*H3*), 7.24 (d, 1 H, Ar*H5*) ppm.

[Fe(acac)L1]$_2$·MeCN (1): Complex **1** was prepared by dissolving H_2L1 (1.0 mmol) and Fe(acac)$_3$ (1.0 mmol) in 40 mL of dry acetonitrile. The dark red solution was stirred until all starting materials dissolved. The resulting solution was kept at room temperature for 1 week, leading to brown X-ray quality crystals. The crystals were filtered off and dried in air; yield 90 mg (10%). $C_{48}H_{75}Fe_2N_3O_8$ (933.81): calcd. C 61.74, H 8.10, N 4.50; found C 61.24, H 7.91, N 4.27.

[FeClL1]$_2$ (2): Complex **2** was prepared by mixing with continuous stirring a solution of H_2L1 (147 mg, 0.5 mmol) in 30 mL of acetonitrile with another solution of $FeCl_3$ (82 mg, 0.5 mmol) in 30 mL of acetonitrile. The resulting dark red-brown olution was kept at room temperature for 2 weeks, leading to dark brown/red X-ray quality crystals. The crystals were filtered off and dried in air; yield 122 mg (32%). $C_{36}H_{58}Cl_2Fe_2N_2O_4$ (765.45): calcd. C 56.49, H 7.64, N 3.66; found C 56.06, H 7.31, N 3.64.

[FeClL2]$_2$ (3): Complex **3** was prepared by mixing with continuous stirring a solution of H_2L2 (154 mg, 0.5 mmol) in 25 mL of acetonitrile with another solution of $FeCl_3$ (82 mg, 0.5 mmol) in 25 mL of acetonitrile. The resulting dark red solution was kept at room temperature for 3 d, leading to dark red, X-ray quality crystals. The crystals were filtered off and dried in air; yield 49 mg (13%). $C_{34}H_{54}Cl_2Fe_2N_2O_4$ (737.40): calcd. C 55.38, H 7.38, N 3.80; found C 55.08, H 7.19, N 3.70.

X-ray Crystallography: Crystals suitable for single-crystal X-ray measurements were obtained directly from the reaction vessels. The crystal data for compounds **1**–**3** are summarized in Table 5 along with other experimental details. The crystallographic data were collected at 123 K (structures **1** and **3**) or 173 K (structure **2**) with an Enraf Nonius Kappa CCD area-detector diffractometer with the use of graphite-monochromated Mo-K_α radiation (λ = 0.71073 Å). Data collection was performed by using ϕ and ω scans, and the data were processed by using DENZO-SMN v0.93.0.[14] SADABS[15] absorption correction was applied for compounds. The structures were solved by direct methods by using the SHELXS-97[16] program or the SIR-97[17] program and full-matrix least-squares refinements on F^2 were performed using the SHELXL-97[16] program. Figures were drawn with ORTEP-3 for Microsoft Windows®.[18] For all compounds the heavy atoms were refined anisotropically. The CH hydrogen atoms were included at the calculated distances with fixed displacement parameters from their host atoms (1.2 times of the host atom).

Table 5. Summary of crystallographic data for **1**–**3**.

	1	**2**	**3**
Formula	$C_{48}H_{75}Fe_2N_3O_4$	$C_{36}H_{58}Cl_2Fe_2N_2O_4$	$C_{34}H_{54}Cl_2Fe_2N_2O_4$
M_r	933.81	765.44	737.40
Crystal syst.	monoclinic	monoclinic	triclinic
Space group (no.)	*C*2/*c* (15)	$P2_1/c$ (14)	$P\bar{1}$ (2)
a [Å]	20.4842(10)	11.8804(6)	10.1562(3)
b [Å]	9.09400(29)	9.9248(5)	11.3655(3)
c [Å]	27.4012(13)	33.9254(16)	16.5073(5)
α [°]	90	90	95.8785(17)
β [°]	102.579(5)	99.1893(15)	89.3037(17)
γ [°]	90	90	93.6103(23)
V [Å]	4981.8(4)	3948.8(3)	1891.63(9)
Z	4	4	2
D_c [g cm^{-1}]	1.245	1.288	1.295
μ(Mo-K_α) [mm^{-1}]	0.634	0.907	0.944
T [K]	123(2)	173(2)	123(2)
Observed refl.	12706	17419	24864
R_{int}	0.0537	0.0427	0.0943
Parameters	287	460	417
R_1[a]	0.086 (0.061)[b]	0.063 (0.047)	0.134 (0.091)
wR_2[c]	0.147 (0.135)	0.131 (0.123)	0.238 (0.216)
Largest difference peak / hole [e Å^{-3}]	1.088 / –0.368	0.459 / –0.569	1.901 / –0.854

[a] $R_1 = \Sigma||F_o| - |F_c||/\Sigma|F_o|$. [b] Values in parentheses: reflections with $I > 2\sigma(I)$. [c] $wR_2 = \{\Sigma[w(F_o^2 - F_c^2)^2]/\Sigma[w(F_o^2)^2]\}^{1/2}$ and $w = 1/[\sigma^2(F_o^2) + (aP)^2 + (bP)]$, where $P = (2F_c^2 + F_o^2)/3$.

CCDC-797577 (for **1**), -797578 (for **2**), -797579 (for **3**), contain the supplementary crystallographic data for this paper. These data can be obtained free of charge from The Cambridge Crystallographic Data Centre via www.ccdc.cam.ac/uk/data_request/cif

Computational Details: All theoretical calculations were carried out at the DFT level of theory using the hybrid B3LYP exchange-correlation functional[19] as implemented in the Gaussian 03 program.[20] A quadratic convergence method was employed in the SCF process.[21] The triple-ζ quality basis set proposed by Ahlrichs and coworkers has been used for all atoms.[22] Calculations were performed on the complexes built from the experimental geometries. The electronic configurations used as starting points were created using Jaguar 7.6 software.[23] The approach used to determine the exchange coupling constants for polynuclear complexes has been described in detail elsewhere.[24]

Supporting Information (see footnote on the first page of this article): The spin density of compound **3** is given in Figure S1.

Acknowledgments

We are grateful to Elina Hautakangas for performing elemental analyses. This work was supported by the Spanish Ministry of Education (MEC) (project number CTQ-2008-02269/BQU), the Junta

de Andalucía (FQM-195 and Project of excellence FQM-3705). We would like to thank the Centro de Supercomputación de la Universidad de Granada for computational resources. The authors are also grateful to Dr. Joan Cano, University of Valencia, Spain, for his continuous and generous assistance with the DFT calculations.

[1] a) R. R. Chrichton, *Inorganic Biochemistry of Iron Metabolism*, Ellis Horwood, Chichester, **1991**; b) I. Bertini, H. B. Gray, S. J. Lippard, J. S. Valentine, *Bioinorganic Chemistry*, University Science Book, Mill Valley, **1994**; c) A. X. Trautwein (Ed.), *Bioinorganic Chemistry: Transition Metals in Biology and their Coordination Chemistry*, DFG-Report zum Schwerpunktprogramm Bioanorganische Chemie, Wiley-VCH, Weinheim, Germany, **1997**; J. DuBois, T. J. Mizoguchi, S. Lippard, *J. Coord. Chem. Rev.* **2000**, *200–202*, 443; E. I. Solomon, T. C. Brunold, M. I. Davis, J. N. Kemsley, S.-K. Lee, N. Lehnert, F. Neese, A. J. Skulan, Y.-S. Yang, J. Zhou, *Chem. Rev.* **2000**, *100*, 235.

[2] F. Le Gall, F. F. Biani, A. Caneschi, P. Cinelli, A. Cornia, A. C. Fabretti, D. Gatteschi, *Inorg. Chim. Acta* **1997**, *262*, 123.

[3] M. Gorun, S. J. Lippard, *Inorg. Chem.* **1991**, *30*, 1625.

[4] R. Werner, S. Ostrovsky, K. Griesar, W. Haase, *Inorg. Chim. Acta* **2001**, *326*, 78.

[5] For some recent reviews, see: a) G. Christou, D. Gatteschi, D. N. Hendrickson, R. Sessoli, *MRS Bull.* **2000**, *25*, 66; b) D. Gatteschi, R. Sessoli, *Angew. Chem. Int. Ed.* **2003**, *42*, 268; c) G. Christou, *Polyhedron* **2005**, *24*, 2065; d) D. Gatteschi, R. Sessoli, J. Villain, *Molecular Nanomagnets*; Oxford University Press: Oxford, UK, **2006**; e) G. Aromí, E. K. Brechin, *Struct. Bonding (Berlin)* **2006**, *122*, 1; J.-N. Rebilly, T. Mallah, *Struct. Bonding (Berlin)* **2006**, *122*, 103; f) A. Cornia, A. F. Costantino, L. Zobbi, A. Caneschi, D. Gatteschi, M. Mannini, R. Sessoli, *Struct. Bonding (Berlin)* **2006**, *122*, 133; g) C. J. Milios, S. Piligkos, E. K. Brechin, *Dalton Trans.* **2008**, 1809.

[6] a) J. I. Ball, C. H. Morgan, *Acta Crystallogr.* **1967**, *23*, 239; b) J. Yoshida, S. Nishikiori, R. Kuroda, *Chem. Eur. J.* **2008**, *14*, 10570.

[7] a) R. van Gorkum, J. Berding, A. M. Mills, H. Kooijman, D. M. Tooke, A. L. Spek, I. Mutikainen, U. Turpeinen, J. Reedijk, E. Bouwman, *Eur. J. Inorg. Chem.* **2008**, 1487; b) A. Neves, L. M. Rossi, I. Vencato, W. Haase, R. Werner, *J. Chem. Soc., Dalton Trans.* **2000**, 707; c) A. Neves, M. A. de Brito, I. Vencato, V. Drago, K. Griesar, W. Haase, *Inorg. Chem.* **1996**, *35*, 2360.

[8] A. W. Addison, T. N. Rao, J. Reedijk, J. van Rijn, G. C. Verschcoor, *J. Chem. Soc., Dalton Trans.* **1984**, 1349.

[9] S. H. Weihe, H. U. Güdel, *J. Am. Chem. Soc.* **1997**, *119*, 6539.

[10] a) O. Wichmann, H. Sopo, E. Colacio, A. Mota, R. Sillanpää, *Eur. J. Inorg. Chem.* **2009**, 4877; b) D. Venegas-Yazigia, D. Aravena, E. Spodine, E. Ruiz, S. Alvarez, *Coord. Chem. Rev.* **2010**, *254*, 2086.

[11] E. Ruiz, J. Cirera, S. Alvarez, *Coord. Chem. Rev.* **2005**, *249*, 2649.

[12] T. Moeller (Ed.), *Inorganic Syntheses*, vol. V, McGraw Hill Book Company, **1957**.

[13] A. Riisiö, O. Wichmann, R. Sillanpää, *Lett. Org. Chem.* **2010**, 298.

[14] Z. Otwinowski, W. Minor, in: *Methods in Enzymology*, Part A (Eds.: C. W. Carter, R. M. Sweet), Academic Press, New York, **1997**, vol. 276, pp. 307–326.

[15] G. M. Sheldrick, *SADABS*, University of Göttingen, Germany, **2002**.

[16] G. M. Sheldrick, *SHELXS-97 and SHELXL-97: A Program for Crystal Structure Refinement*, University of Göttingen, Germany, **1997**.

[17] A. Altomare, M. Cascarano, C. Giacovazzo, A. Guagliardi, M. C. Burla, G. Pilodori, M. Camalli, *J. Appl. Crystallogr.* **1994**, *27*, 435.

[18] L. J. Farrugia, *J. Appl. Crystallogr.* **1997**, *30*, 565.

[19] a) A. D. Becke, *Phys. Rev. A* **1988**, *38*, 3098; b) C. T. Lee, W. T. Yang, R. G. Parr, *Phys. Rev. B* **1988**, *37*, 785; c) A. D. Becke, *J. Chem. Phys.* **1993**, *98*, 5648.

[20] M. J. Frisch, G. W. Trucks, H. B. Schlegel, G. E. Scuseria, M. A. Robb, J. R. Cheeseman, J. A. Montgomery Jr., T. Vreven, K. N. Kudin, J. C. Burant, J. M. Millam, S. S. Iyengar, J. Tomasi, V. Barone, B. Mennucci, M. Cossi, G. Scalmani, N. Rega, G. A. Petersson, H. Nakatsuji, M. Hada, M. Ehara, K. Toyota, R. Fukuda, J. Hasegawa, M. Ishida, T. Nakajima, Y. Honda, O. Kitao, H. Nakai, M. Klene, X. Li, J. E. Knox, H. P. Hratchian, J. B. Cross, C. Adamo, J. Jaramillo, R. Gomperts, R. E. Stratmann, O. Yazyev, A. J. Austin, R. Cammi, C. Pomelli, J. W. Ochterski, P. Y. Ayala, K. Morokuma, G. A. Voth, P. Salvador, J. J. Dannenberg, V. G. Zakrzewski, S. Dapprich, A. D. Daniels, M. C. Strain, O. Farkas, D. K. Malick, A. D. Rabuck, K. Raghavachari, J. B. Foresman, J. V. Ortiz, Q. Cui, A. G. Baboul, S. Clifford, J. Cioslowski, B. B. Stefanov, G. Liu, A. Liashenko, P. Piskorz, I. Komaromi, R. L. Martin, D. J. Fox, T. Keith, M. A. Al-Laham, C. Y. Peng, A. Nanayakkara, M. Challacombe, P. M. W. Gill, B. Johnson, W. Chen, M. W. Wong, C. Gonzalez, J. A. Pople, *Gaussian 03*, rev. C.02, Gaussian, Inc., Wallingford CT, **2004**.

[21] G. B. Bacskay, *Chem. Phys.* **1981**, *61*, 385.

[22] A. Schäfer, C. Huber, R. Ahlrichs, *J. Chem. Phys.* **1994**, *100*, 5829.

[23] *Jaguar 7.6*, Schrödinger, Inc., Portland, OR, **2009**.

[24] a) E. Ruiz, J. Cano, S. Alvarez, P. Alemany, *J. Comput. Chem.* **1999**, *20*, 1391; b) E. Ruiz, S. Alvarez, A. Rodríguez-Fortea, P. Alemany, Y. Puoillon, C. Massobrio, in: *Magnetism: Molecules to Materials* (Eds.: J. S. Miller, M. Drillon), Wiley-VCH, Weinheim, Germany, **2001**, vol. II, p. 5572; c) E. Ruiz, A. Rodríguez-Fortea, J. Cano, S. Alvarez, P. Alemany, *J. Comput. Chem.* **2003**, *24*, 982; d) E. Ruiz, S. Alvarez, J. Cano, V. Polo, *J. Chem. Phys.* **2005**, *123*, 164110.

Received: November 15, 2010
Published Online: March 17, 2011

